Calculation of the two-dimensional infrared-active localized modes of a soliton lattice in *trans*-polyacetylene

Z. J. Li, Z. An, and Z. L. Liu
Department of Physics, National Laboratory of Laser Technology, Huazhong University of Science & Technology, Wuhan, China

K. L. Yao
Center of Theoretical Physics, Chinese Center of Advanced Science and Technology (World Laboratory), Beijing, China; Department of Physics, Huazhong University of Science and Technology, Wuhan, China; and International Center for Material Science, Shenyang, 110015, China

(Received 26 July 1993)

Starting from the extensional Su-Schrieffer-Heeger model Hamiltonian containing intrachain e-e interactions, a bond-bending term, and an external Coulomb potential arising from the interchain-charged solitons and counterions, all the two-dimensional vibrational modes around the soliton lattice are calculated for doping levels from $y=3.33$ at. % to $y=16.67$ at. %. Thirteen localized vibrational modes are found for dopant concentrations from 3.33 to 13.33 %, in which seven modes are infrared active and correspond with the infrared absorption peaks. No localized modes have been found for doping levels above $y=16.67$ at. %. In addition, the frequencies of the modes are decreased and their localizations are weakened when the dopant concentrations increase.

I. INTRODUCTION

Since Su, Schrieffer, and Heeger (SSH) proposed the soliton model[1] of polyacetylene, a number of experimental studies and theoretical calculations have been carried out to support this model. Sun, Wu, and Shen[2] and Cohen and Glick[3] have calculated the localized modes around a soliton by using the SSH model or its extensional model and qualitatively explained the infrared absorption. The present authors[4,5] have assessed the influence of polyacetylene configuration on the localized modes of soliton from the two-dimensional (2D) extension of SSH model and found several new 2D infrared-active localized modes. It should be noticed that all the above-mentioned results came out from the pure and dilute doping levels situations, in which the soliton-antisoliton interactions have been neglected. With the increasing of the dopant concentration, the spacing between solitons gets comparable to the width of a soliton, and their coherent actions could not be ignored. Stafström[6] and Conwell, Mizes, and Jeyadev[7] have investigated the possibility of the soliton lattice in highly doped polyacetylene as viewed from the energy band. In this paper, we will investigate the 2D localized modes around a soliton lattice by using the 2D extensional SSH model.

II. METHOD OF CALCULATION

The Hamiltonian employed for the soliton lattice contains the following terms:

$$H=H_{\mathrm{SSH}}+H_{e-e}+H_c \ , \tag{1}$$

where

$$H_{\mathrm{SSH}}=-\sum_{n,\sigma}(t_0-\alpha\delta r_{n+1,n})(c^{+}_{n+1,\sigma}c_{n,\sigma}+\mathrm{H.c.}) +\frac{k}{2}\sum_n(\delta r_{n+1,n})^2+\frac{k'}{2}\sum_n(\delta\theta_n)^2 +\frac{M}{2}\sum_n(\dot{\mathbf{r}})^2 \tag{2}$$

all the notations have the conventional meanings:[4,5]

$$H_{e-e}=\frac{1}{2}U\sum_{n,\sigma}C^{+}_{n,\sigma}C_{n,\sigma}C^{+}_{n,-\sigma}C_{n,-\sigma} \ , \tag{3}$$

U is the interaction parameter of Hubbard repulsion. We take $U=1.25$ eV in our calculation:

$$H_c=\sum_{n,\sigma}(V_n^{\mathrm{imp}}+V_n^{\mathrm{sol}})C^{+}_{n,\sigma}C_{n,\sigma} \ , \tag{4}$$

where V_n^{imp} is the Coulomb potential at site n due to the counterions, and V_n^{sol} is the potential due to the charges on surrounding chains:

$$V_n^{\mathrm{imp}}=-e^2\sum_{n_j}\frac{1-v_{nn_j}(1-e^{-\gamma|n-n_j|a})}{\epsilon_\perp[(n-n_j)^2a^2+(\epsilon_\parallel/\epsilon_\perp)d_1^2]^{1/2}} \ , \tag{5}$$

$$V_n^{\mathrm{sol}}=e^2\sum_{n'}\frac{1-v_{nn'}(1-e^{-\gamma|n-n'|a})}{\epsilon_\perp[(n-n')^2a^2+(\epsilon_\parallel/\epsilon_\perp)d_2^2]^{1/2}} \ . \tag{6}$$

Here $a=1.222$ Å is the average distance between adjacent sites along the chain axis, $d_1=2.4$ Å is the perpendicular distance of the impurity from the chain, $d_2=\sqrt{3}d_1$ is the perpendicular distance between adjacent chains, n_j is the displacement of the counterions along the surrounding

 ©1994 The American Physical Society

chain, and n' is the displacement of the solitons in the surrounding chains. $\epsilon_\perp$ and $\epsilon_\parallel$ are the dielectric constants, and equal to 11.5 and 2.5. The exponential screening in Eqs. (5) and (6) is controlled by the two parameters γ and $v_{nn_j}(v_{nn'})$,[6,7] where $\gamma=0.373$ Å^{-1}, $v_{nn_j}=\min(|n-n_j|/l_c,l)$, and l_c is the spacing between the neighbor counterions in the unit of C-C bonds.

A static solution of the soliton lattice can be determined by the following self-consistent equations:

$$\begin{aligned}\varepsilon_i^\sigma\psi_i^\sigma(n)=&-(t_0-\alpha\delta\mathbf{r}_{n,n-1})\psi_i^\sigma(n-1)\\&-(t_0-\alpha\delta\mathbf{r}_{n+1,n})\psi_i^\sigma(n+1)\\&+[V(n)+U\chi_{n,\sigma}]\psi_i^\sigma(n)\ ,\\ \chi_{n,\sigma}=&\sum_{\substack{i,\sigma\\(\mathrm{occ})}}\psi_i^{-\sigma}(n)\psi_i^{-\sigma}(n)\ ,\end{aligned}\tag{7}$$

$$\delta\mathbf{r}_{n+1,n}=\frac{2\alpha}{K}\left[\sum_{\substack{\sigma\\(\mathrm{occ})}}\psi_i^\sigma(n+1)\psi_i^\sigma(n)-\frac{1}{N}\sum_{\substack{n,i,\sigma\\(\mathrm{occ})}}\psi_i^\sigma(n+1)\psi_i^\sigma(n)\right],$$

where the periodic boundary conditions have been used. $V(n)=V_n^{\mathrm{imp}}+V_n^{\mathrm{sol}}$, ε_i^σ is the eigenvalue of electron with spin σ, and $\psi_i^\sigma(n)$ denotes the nth component of electron eigenfunction with spin σ.

Now, we consider the small vibration around the soliton lattice, expanding $\delta r_{n+1,n}$ near the equilibrium configuration $\{\delta r^s_{n+1,n}\}$ (Refs. 4 and 5):

$$\begin{aligned}\delta\mathbf{r}_{n+1,n}=&\sin\theta(x_{n+1}-x_n)\\&+(-1)^{n+1}\cos\theta(y_{n+1}-y_n)+\delta r^s_{n+1,n}\ ,\end{aligned}\tag{8}$$

where θ is half of the bond angle and the coordinate is chosen as in Ref. 5. The direction of chain is defined as x, the normal direction is y. Then the total energy can be written as

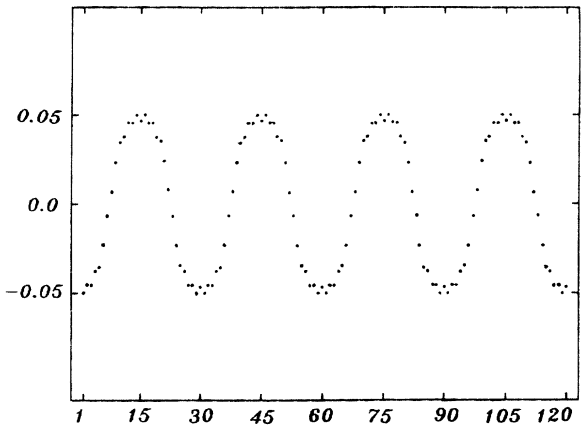

FIG. 1. The solitons configuration at doping level $y=6.67$ at. % ($N_g=8$).

$$E=E^s+\frac{1}{2}\sum_{m,n}V_{mn}^{\alpha\beta}\eta_m^\alpha\eta_n^\beta+\frac{M}{2}\sum_n(\dot{\mathbf{r}}_n)^2\ ,\tag{9}$$

where $\alpha,\beta=1,2$ denote the x and y directions, respectively. E^s is the static energy of the soliton lattice. Readers are referred to Ref. 5 for an explicit expression of $V_{mn}^{\alpha\beta}$.

III. RESULTS AND DISCUSSION

In the following calculation, we take the ring with 120 carbon atoms, and the doping regime is from $y=3.33$ at. % to $y=16.67$ at. %, corresponding to the soliton number from $N_g=4$ to $N_g=20$. The parameters appearing in SSH Hamiltonian are $K=21$ eV/Å^2, $k'=1.5$ eV, $t_0=2.5$ eV, and $\alpha=4.1$ eV/Å. Solving self-consistent equations (7), the geometry optimizations and the energy spectra are obtained. The results show that the electronic states of solitons are extended states and the soliton energy levels change to soliton energy bands. The optimized solitons configurations at doping level $y=6.67$ at. % ($N_g=8$) are plotted in Fig. 1.

Our calculations (see Table I) show that 13 localized

TABLE I. Frequencies of the localized modes around a soliton lattice for different dopant concentrations. Here $\omega_Q=(4\ \mathbf{K}/\mathbf{M})^{1/2}$ is the bare frequency.

Modes	Parity	Frequencies (ω^2/ω_Q^2) $N_s=4$ (3.33%)	$N_s=6$ (5.00%)	$N_s=8$ (6.67%)	$N_s=10$ (8.33%)	$N_s=12$ (10.00%)	$N_s=16$ (13.33%)
G_1	Even	0.0530	0.0530	0.0528	0.0526	0.0524	0.0522
G_2	Odd	0.0532	0.0532	0.0531	0.0530	0.0529	0.0527
G_3	Even	0.2332	0.2136	0.2014	0.1854	0.1721	0.1634
G_4	Odd	0.2351	0.2146	0.2019	0.1925	0.1864	0.1671
G_5	Even	0.2389	0.2167	0.2052	0.2026	0.2035	0.2025
G_6	Odd	0.2397	0.2198	0.2092	0.2131	0.2211	0.2126
G_7	Even	0.2549	0.2252	0.2130	0.2237	0.2373	0.2306
G_8	Odd	0.2622	0.2311	0.2172	0.2438	0.2807	0.2585
G_9	Even	0.3655	0.3641	0.3626	0.3615	0.3607	0.3602
G_{10}	Odd	0.3658	0.3645	0.3629	0.3617	0.3609	0.3606
G_{11}	Even	0.4474	0.4467	0.4061	0.4044	0.4022	0.3943
G_{12}	Even	0.5080	0.5030	0.4974	0.4834	0.4755	0.4729
G_{13}	Odd	0.5080	0.5021	0.4936	0.4916	0.4765	0.4735

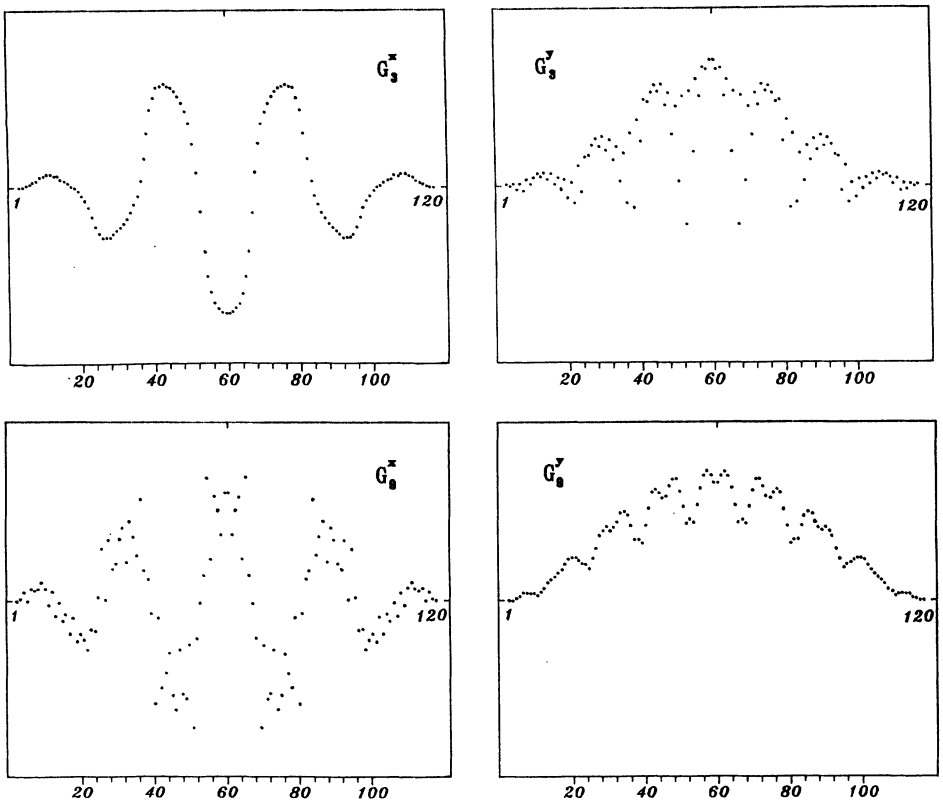

FIG. 2. The shapes of the localized modes G_9 and G_i for the doping level $y=6.67$ at.% ($N_9=8$). The unit of the abscissa is site number n, and the ordinate is an arbitrary unit. (a) and (b) correspond to G_3 and G_9, respectively.

modes have been found at doping levels from $y=3.33$ at.% to $y=13.33$ at.%, and no localized modes occur from doping level above $y=16.67$ at.%. The modes G_1, G_3, G_6, G_7, G_9, G_{11}, and G_{12} have even symmetry, related to the infrared absorption. G_2, G_4, G_6, G_8, G_{10}, and G_{13} have odd symmetry, and are Raman active. The shapes of G_3 and G_9 at doping level $y=6.67$ at.% ($N_g=8$) are plotted in Fig. 2. Furthermore, all the frequencies of localized modes are decreased and the localizations are weakened when the dopant concentration increases.

Finally, we would like to make some comparisons of our results with the experimental data. At the dilute doping levels, the three characteristic infrared lines at 930, 1288, and 1400 cm^{-1} along with a weaker peak at 1215 cm^{-1} have been well known.[8] At high-doping levels, the four (three stronger and one weaker) infrared absorption peaks, which are red shifted to 487, 1284, 1362, and 1000 cm^{-1}, have been observed (shown in Fig. 3).[9] In addition, two smaller peaks (a and b) near the 487 cm^{-1} peak have been found too (see Fig. 3). In our calculation, when bare frequency[3] $\omega_Q=(4\ K/M)^{1/2}\simeq 2140$

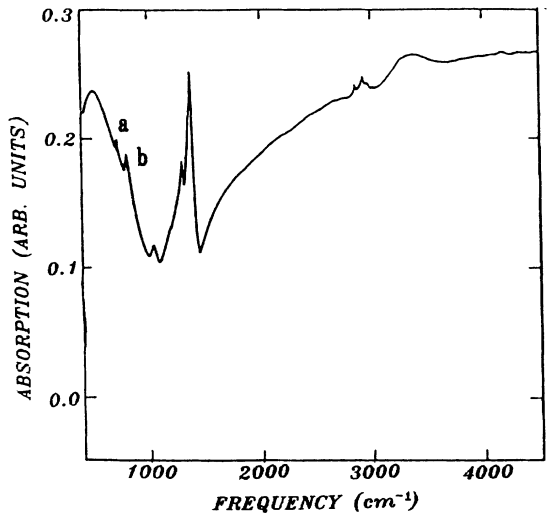

FIG. 3. The infrared absorption spectrum at doping level $y=6$ at.%.

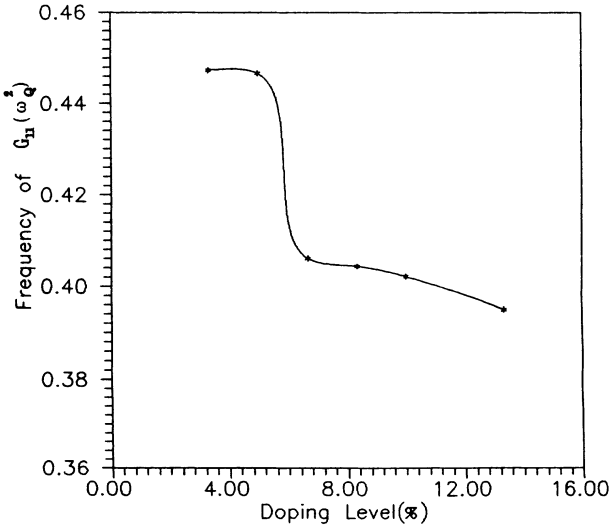

FIG. 4. The frequency of the mode G_{11} as a function of the dopant concentration.

cm^{-1}, the frequencies of the infrared active modes are $\omega_1=490$ cm^{-1}, $\omega_3=957$ cm^{-1}, $\omega_5=965$ cm^{-1}, $\omega_7=984$ cm^{-1}, $\omega_9=1284$ cm^{-1}, $\omega_{11}=1359$ cm^{-1}, and $\omega_{12}=1503$ cm^{-1} at doping level $y=6.67$ at. %. Thus, while the modes G_1, G_9, and G_{11} correspond to the three strong absorption lines, the modes G_3, G_5, and G_7 accord with the two smaller peaks and the weaker peak, respectively. Although the mode G_{12} is also infrared active, it might be too weak for infrared absorption to be observed in the experiments. Besides, the frequency of the mode G_{11} decreases abruptly between 5.00 at. % and above 6.67 at. %, which is quite similar to that observed by Ehrenfreund.[10] The frequency of G_{11} as the function of y is plotted in Fig. 4. Therefore, the seven infrared-active modes can be used to interpret observed absorption lines.

IV. CONCLUSION

Thirteen 2D localized vibrational modes around the soliton lattice have been found until the dopant concentration $y=13.33$ at. %, and seven of them are IRAV modes, which are agreement with experimental data. Based on the results, we can propose that the soliton lattice could play an important role in both the middle-doped polyacetylene and the highly doped one.

ACKNOWLEDGMENT

This project was supported by the National Natural Science Foundation of China.

[1]P. W. Su, J. R. Schrieffer, and A. J. Heeger, Phys. Rev. B **22**, 2099 (1980).
[2]X. Sun, C. Wu, and X. Shen, Solid State Commun. **56**, 1039 (1985).
[3]Richard J. Cohen and Arnold J. Glick, Phys. Rev. B **36**, 2907 (1987).
[4]Z. J. Li, Z. An, K. L. Yao, and Z. G. Li, Z. Phys. B **91**, 221 (1993).
[5]Z. J. Li, Biao Xing, and K. L. Yao, Phys. Rev. B **44**, 5029 (1991).
[6]S. Stafström, Phys. Rev. B **43**, 9158 (1991).
[7]E. M. Conwell, H. A. Mizes, and S. Jeyadev, Phys. Rev. Lett. **61**, 361 (1988); Phys. Rev. B **40**, 1630 (1989).
[8]G. Blanchet *et al.*, Phys. Rev. Lett. **50**, 1938 (1983).
[9]Y. H. Kim and A. J. Heeger, Phys. Rev. B **40**, 8393 (1989).
[10]E. Ehrenfreund, Z. Vardeny, and O. Brafman, Phys. Rev. Lett. **57**, 2081 (1986).